X-ray resonant scattering determination of the antiferroquadrupolar ordering in UPd_3 at low temperatures

2008 J. Phys.: Condens. Matter 20 395221

(http://iopscience.iop.org/0953-8984/20/39/395221)

J. Phys.: Condens. Matter **20** (2008) 395221 (7pp) doi:10.1088/0953-8984/20/39/395221

X-ray resonant scattering determination of the antiferroquadrupolar ordering in UPd_3 at low temperatures

H C Walker[1], K A McEwen[1], M D Le[1], L Paolasini[2] and D Fort[3]

[1] London Centre for Nanotechnology and Department of Physics and Astronomy, University College London, Gower Street, London WC1E 6BT, UK
[2] European Synchrotron Radiation Facility, BP200, F-38043 Grenoble Cedex, France
[3] Department of Metallurgy, University of Birmingham, Birmingham B15 2TT, UK

E-mail: helen.walker@ucl.ac.uk

Received 24 April 2008
Published 4 September 2008
Online at stacks.iop.org/JPhysCM/20/395221

Abstract

We have used x-ray resonant scattering techniques to make a comprehensive study of the quadrupolar order in UPd_3. New measurements reveal that the order parameter describing the in-phase stacking along the c-axis of the quadrupole moments of the uranium ions on the quasi-cubic sites is primarily Q_{xy} in the two lowest temperature phases. These results are discussed within the context of a three-level crystal field model for the uranium $5f^2$ electrons, the allowed quadrupolar operators, and the constraints deduced from the analysis of heat capacity measurements. We have now deduced, and summarize, the order parameters for each of the four antiferroquadrupolar phases of UPd_3.

(Some figures in this article are in colour only in the electronic version)

1. Introduction

There has recently been a great deal of interest in the interplay of spin and lattice degrees of freedom resulting in intriguing physical phenomena [1], for example: orbital ordering in the transition metal oxides [2], Jahn–Teller distortions [3], multipolar order in f electron systems such as quadrupolar order in CeB_6 [4] and magnetic triakontadipolar (rank 5) order in NpO_2 [5], and heavy fermion behaviour with proposed hidden order in $PrFe_4P_{12}$ [6]. The study of multipolar interactions concerning the unfilled f electrons in the rare-earth and actinide intermetallics involves the complex problems of pair interactions between different ions and the effect of the crystal field acting on an f ion. The quadrupolar interaction is mediated by the conduction electrons via an indirect mechanism similar to the RKKY interaction. When this coupling dominates the magneto-elastic coupling, quadrupolar order may occur and the ordering can be either ferro- or antiferroquadrupolar depending on the sign of the pair interaction [7]. UPd_3 is a canonical example of an intermetallic compound that exhibits antiferroquadrupolar order. Unusually, it displays four different quadrupolar transitions. Using x-ray resonant scattering (XRS) techniques we have previously determined the highest temperature quadrupolar phase as being described primarily by the Q_{zx} order parameter [8]. In the present paper, we report new measurements performed in the two lowest temperature phases.

UPd_3 has the $TiNi_3$ structure (space group $P6_3/mmc$, lattice parameters $a = 5.73$ Å, $c = 9.66$ Å), i.e. double-hexagonal close-packed. The uranium ions are stacked in layers with the sequence ABACABAC, such that there are two inequivalent uranium sites, with locally hexagonal and quasi-cubic site symmetry, respectively [9]. The inter-uranium distance is 4.11 Å, which is greater than the Hill limit and hence the 5f electrons are localized, as is demonstrated by the observation of well defined crystalline electric field excitations on both uranium sites [10]. Quadrupolar ordering of the uranium ions in UPd_3 was first identified with the discovery, in neutron diffraction studies, of weak superlattice reflections at $(\frac{1}{2}, 0, l)$ in hexagonal notation, or in orthorhombic notation, at $(1, 0, l)$ [11], see figure 1. Since then this hypothesis has been supported by numerous macroscopic (heat capacity [12, 13, 8], magnetic susceptibility [14], thermal expansion [15], ultrasonics [16]) and microscopic

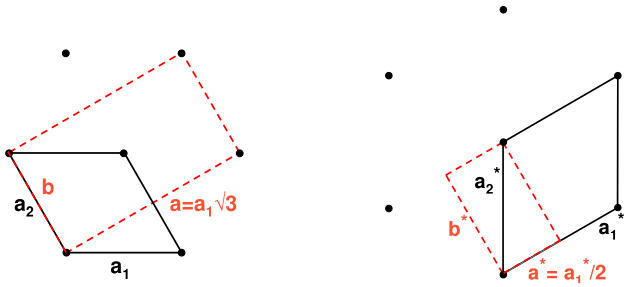

(a) Real space (b) Reciprocal space

Figure 1. The hexagonal (solid (black) line) and orthorhombic (dashed (red) line) unit cells drawn in the basal plane in real and reciprocal space, showing how the two cells are geometrically related.

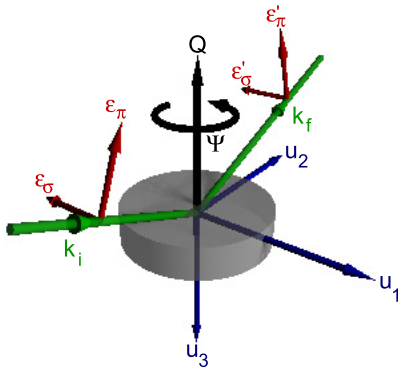

Figure 2. Schematic representation of the experimental setup to perform azimuthal dependent XRS studies, where **u** are the basis vectors describing the reference frame, $\mathbf{k}_i$ and $\mathbf{k}_f$ are the wavevectors of the incident and scattered x-rays. The directions of the sigma and pi polarization vectors are also shown.

(neutron [17] and x-ray diffraction [18, 8]) measurements. The four transitions: $T_0 = 7.8$ K, $T_{+1} = 6.9$ K, $T_{-1} = 6.7$ K and $T_2 = 4.4$ K, can be explained within a crystal field model requiring a doublet ground state on the quasi-cubic sites [14]. We attribute them to a succession of different antiferroquadrupolar ordered structures of the localized uranium $5f^2$ electrons on these quasi-cubic sites. The quadrupolar moments express the deviation of the 5f charge clouds from a perfect spherical distribution. The quadrupolar phase transitions are very sensitive to doping Pt for Pd [15], while quadrupolar order is still observed for up to 5% Np in (U, Np)Pd_3 [19].

Based on polarized neutron diffraction (PND) data [17] and the initial x-ray resonant scattering (XRS) data [18], a scheme for the successive quadrupolar transitions was proposed [14] in which the T_0 transition was ascribed to the $Q_{x^2-y^2}$ order parameter. However, developments in cryostat technology enabled us to perform new XRS experiments in 2005, revealing that the primary order parameter of the first quadrupolar ordered phase below T_0 was in fact Q_{zx} [8], which provides a clear explanation for the observed orthorhombic distortion. The apparent discrepancy between the results from the XRS and PND experiments is, however, illusory. Careful consideration of the matrix elements for the two order parameters reveals that they have the same symmetry. Therefore, when the Q_{zx} order parameter becomes non-zero, a finite $Q_{x^2-y^2}$ order parameter will be induced [10]. At 7 K the best fit to the azimuthal data gives the order parameters Q_{zx} and $Q_{x^2-y^2}$ in the ratio 6:1. PND is not able to probe quadrupolar order directly, but instead the quadrupolar structure is inferred from the measured magnetic (dipolar) structure induced by the application of a magnetic field. In the configuration of the PND experiment reported in [17], with a magnetic field applied parallel to the (real-space) a-axis, only the $Q_{x^2-y^2}$ quadrupoles give rise to an antiferromagnetic structure. Hence the primary Q_{zx} component of the order parameter was not detected.

2. Experimental details

Large resonant enhancements of x-ray magnetic scattering intensities were first observed in holmium metal [20], on tuning the x-ray energy through the Ho L_{III} absorption edge. Since then, signal enhancement has been observed at the K, L and M absorption edges of different elements, and x-ray resonant scattering has been observed in non-magnetic systems displaying orbital order [21] and other forms of electromagnetic multipolar order [22, 23]. The huge increase in signal to noise ratio at resonance has allowed a large variety of problems, previously thought intractable, to be studied.

Resonant behaviour occurs when the incident photon energy is equal to the energy difference between the ground state and an intermediate state, making resonant scattering a direct experimental probe of intermediate atomic states, and as such sensitive to the magnetization of d and f bands, or their splitting due to multipolar interactions. In general, for polarized electromagnetic radiation incident on a system with an anisotropic charge distribution described by a tensor scattering factor $T(r)$, the anomalous atomic scattering factor contains a term

$$f \propto \epsilon' \cdot \tilde{T}(Q) \cdot \epsilon, \tag{1}$$

where $\epsilon^{(\prime)}$ is the polarization vector of the incident (scattered) photon and the scattering factor $\tilde{T}(Q)$ is the Fourier transform of $T(r)$, constructed from the sum over the unit cell of the individual second rank atomic scattering lengths of each ion weighted by the appropriate phase factor. In a quadrupolar ordered system this scattering amplitude is proportional to the electric quadrupole moment [24]. The anisotropic nature of the scattering is observed through the variation of the scattered intensity as a function of the azimuthal angle, Ψ, about the scattering vector, see figure 2. Unlike neutrons, which only couple to the possible lattice distortions induced by quadrupolar ordering, XRS allows us to probe quadrupolar order directly, through a study of the energy, polarization and azimuthal dependence of the intensities of the superlattice reflections.

A single crystal of UPd_3 was grown at the University of Birmingham using the tri-arc Czochralski pulling method [25] starting with 4N palladium and 3N uranium metals. The 200 mg sample was oriented using a Laue camera and cut before polishing with 0.25 μm diamond paste. The

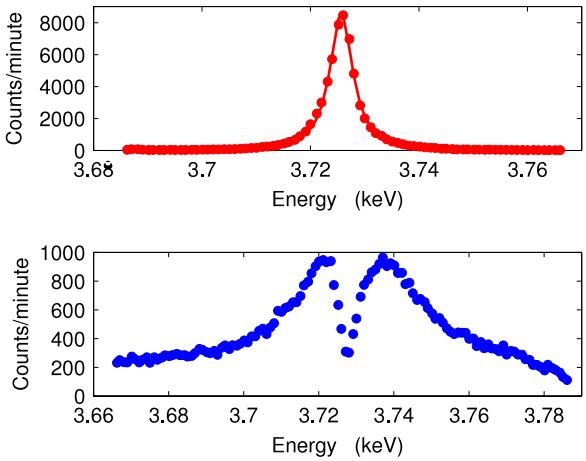

Figure 3. Energy scans of the UPd_3 (104) quadrupolar superlattice reflection at $T = 5.2$ K in the $\sigma\pi$ (upper frame) and $\sigma\sigma$ (lower frame) scattering channels.

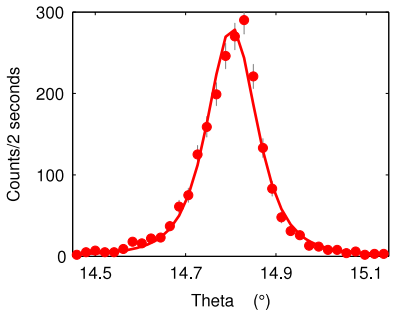

Figure 4. A typical UPd_3 theta rocking curve as measured at (104), $T = 5.2$ K, $E = 3.726$ keV, and $\Psi = 88°$ in the $\sigma\pi$ channel. The solid line corresponds to the least squares fit to a Lorentzian squared function.

experiment was performed on the ID20 magnetic scattering beam line [26] at the European synchrotron radiation facility. The incident x-ray energy was tuned to the uranium M_{IV} absorption edge, $E = 3.726$ keV, where the electric dipole transitions, which dominate the cross-section, connect the core $3d_{3/2}$ states to the 5f states. At this energy only a very small region of reciprocal space is accessible, but this includes two quadrupolar superlattice reflections, which in orthorhombic notation are (103) and (104). These two reflections provide different information about the quadrupolar order. The first measures the component of the anti-phase stacking, and the second the in-phase stacking, of the quadrupole moments along the c-axis, and hence once can investigate different order parameters.

Measurements reported previously [8] studying the phase $T_{+1} < T < T_0$ revealed that the azimuthal dependence of the (103) scattering intensity was predominantly described by the Q_{zx} order parameter, whilst no scattered intensity was observed at (104). In the experiment reported here we focused on the phases $T < T_{-1}$, since it is very difficult to perform the experiments with the prolonged required temperature stability in the second quadrupolar phase between 6.7 and 6.9 K. (Note that a full azimuthal dependence takes over 24 h to measure.) We measured the azimuthal dependence of the (104) intensity over the full 360° of Ψ at $T = 5.2$ and 2.1 K, i.e. in the $T_2 < T < T_{-1}$ and $T < T_2$ quadrupolar phases. For each value of Ψ, the (104) reflection was aligned and then we measured theta rocking curves (where theta is the angle between the incident beam and the planes normal to the scattering vector) with the detector in the rotated ($\sigma\pi$) and unrotated ($\sigma\sigma$) channels, using a gold (111) crystal as the polarization analyser. The azimuthal angle was defined relative to the reference vector [010].

3. Experimental results

After the (104) superlattice reflection was aligned at $T = 5.2$ K, its intensity dependence as a function of incident photon energy was measured in both scattering channels. As shown in figure 3 both channels show a resonant signal, indicating quadrupolar order in the sample (dipolar magnetic order only shows a resonance in $\sigma\pi$ and not $\sigma\sigma$). The resonance in $\sigma\pi$ is very well defined and typical of the M-edge resonance in 5f materials. The line shape can be best fitted using a Lorentzian function, with a peak centre at 3.7257 ± 0.0001 keV. The $\sigma\sigma$ spectrum is more complicated showing some interference with charge scattering.

Figure 4 shows a typical theta rocking curve, where the integrated intensity has been obtained by fitting a Lorentzian squared line shape, which minimizes chi-squared. Using the above procedure for obtaining the integrated intensity, the azimuthal dependence of this integrated intensity of the (104) superlattice reflection in both scattering channels at $T = 5.2$ K was determined and is shown in figure 5. The data has been normalized to the monitor signal to take into account small fluctuations in the x-ray flux incident on the sample. The errorbars correspond to the numerical error obtained from the peak fitting procedure. An estimate of the reproducibility of the data may be obtained by close inspection of figure 5, which shows two overlapping data points at $\Psi = 88°$ in both channels. These two points correspond to the initial and final measured azimuth positions after the cryostat had been rotated through 360°, and as repeat measurements give a more accurate physical estimate of the error in the intensity than the value obtained from the numerical fitting procedure. On this evidence, the reproducibility of our results is most satisfactory.

The measurements were repeated at 2.1 K, i.e. $T < T_2$, and the same data treatment gives the azimuthal dependence of the integrated intensity of the (104) superlattice reflection in the different scattering channels, as shown in figure 6. A comparison of the two data sets shows that this phase demonstrates a very similar azimuthal dependence for the scattering intensity to the higher temperature phase, with the exception of an intensity scaling factor. This approximately two-fold increase in scattered intensity from the (104) superlattice reflection below T_2 is consistent with that observed previously [18].

4. Discussion

To identify the order parameter describing a quadrupolar structure, calculations are performed to determine the

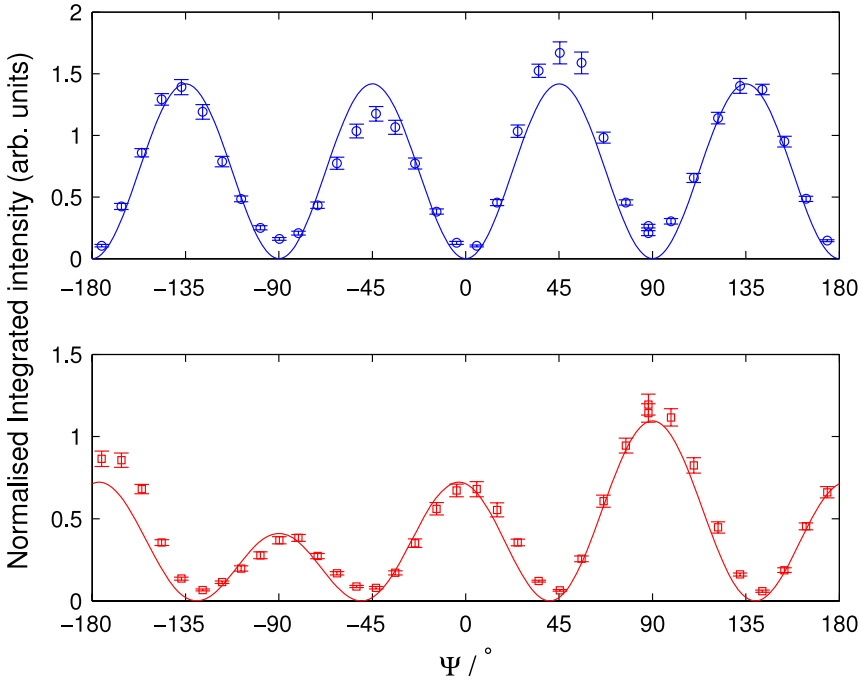

Figure 5. The azimuthal dependence of the $\sigma\sigma$ (○) and $\sigma\pi$ (□) scattering intensities of the (104) peak in UPd_3 at the U M_{IV} edge at $T = 5.2$ K. The solid lines show calculations for the Q_{xy} order parameter.

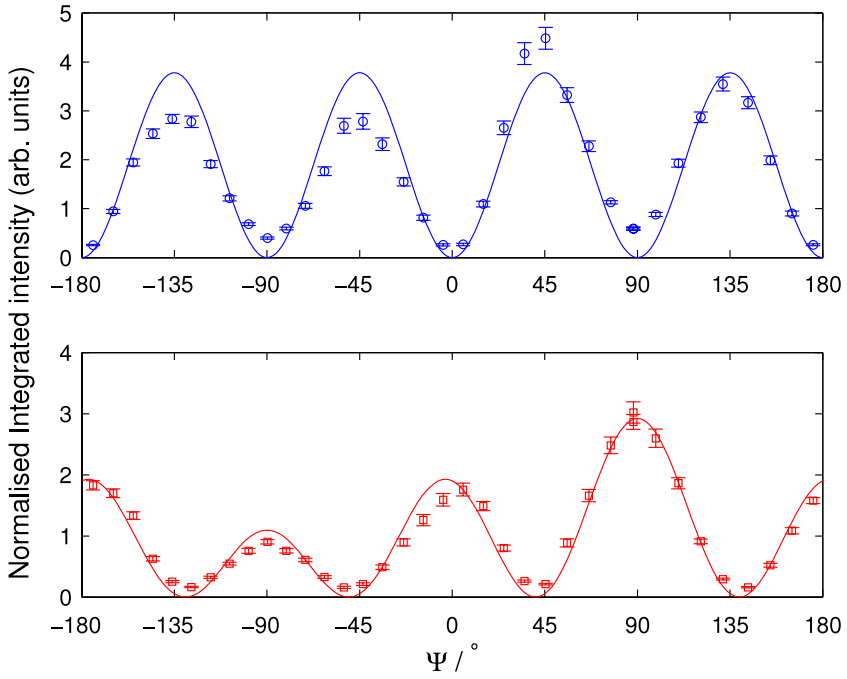

Figure 6. The azimuthal dependence of the $\sigma\sigma$ (○) and $\sigma\pi$ (□) scattering intensities of the (104) peak in UPd_3 at the U M_{IV} edge at $T = 2.1$ K. The solid lines show calculations for the Q_{xy} order parameter.

azimuthal dependence for the given superlattice reflection using equation (1), where the tensor scattering factor is composed of the second rank tensors T_n of the individual uranium quadrupole moments within the unit cell:

$$\tilde{T}(Q) = \sum_n T_n \exp(\imath \mathbf{Q} \cdot \mathbf{r}). \qquad (2)$$

Calculations for the allowed quadrupolar order parameters demonstrate their distinctive features, as can be seen in figure 7.

As shown in figure 5, at 5.2 K within the third quadrupolar phase, the calculated azimuthal dependence of the Q_{xy} order parameter has the same periodicity for the maxima and minima for both scattering channels, and in the case of the $\sigma\pi$

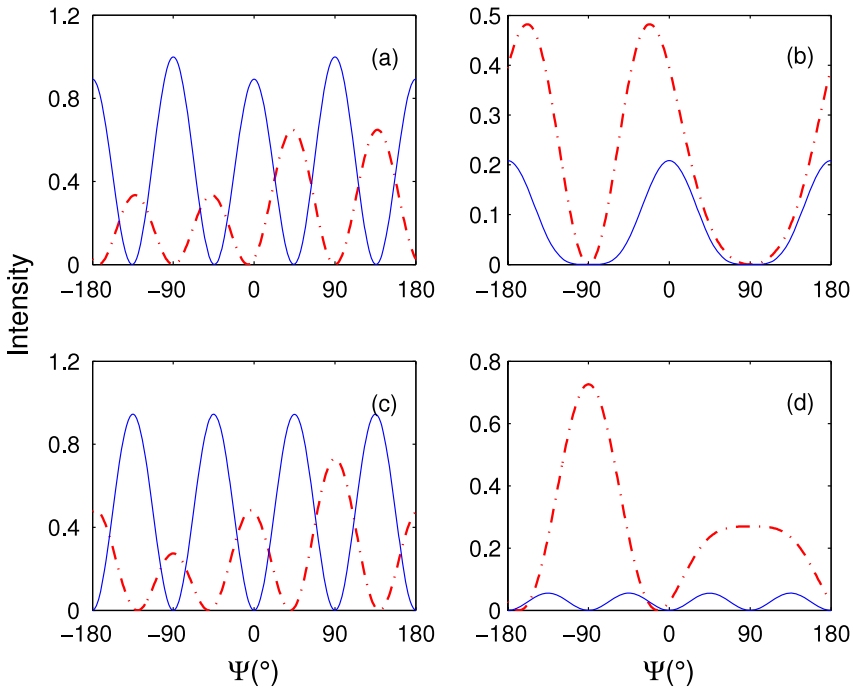

Figure 7. The calculated azimuthal dependence of scattering from the (104) superlattice reflection described by the (a) $Q_{x^2-y^2}$, (b) Q_{zx}, (c) Q_{xy} and Q_{yz} quadrupolar order parameters. The solid (blue) lines, and dot–dashed (red) lines, denote the results for the $\sigma\sigma$ and $\sigma\pi$ channels, respectively.

scattering, the modulation of the heights of the maxima is in excellent agreement with the data. The scattering at (104) arises from the in-phase, or '*ferro*'-component, of the quadrupole stacking along the c-axis, whilst that at (103) is due to the anti-phase, or '*antiferro*', component. In our earlier experiments, we determined that this latter component is described primarily by the Q_{zx} order parameter [8]. Figure 8 is an aid to visualize the quadrupoles on the quasi-cubic uranium sites for these combined order parameters.

As previously reported [8], heat capacity measurements indicate that only the T_{-1} phase transition is strongly first order. Using the three-level model for the lowest crystal field states on the quasi-cubic sites developed by McEwen *et al* [14], the matrices representing the quadrupolar operators can be written as

$$\hat{Q}_{x^2-y^2} = \begin{pmatrix} 0 & A & A \\ A & 0 & B \\ A & B & 0 \end{pmatrix} \qquad \hat{Q}_{zx} = \begin{pmatrix} 0 & A' & A' \\ A' & 0 & B' \\ A' & B' & 0 \end{pmatrix}$$

$$\hat{Q}_{xy} = \begin{pmatrix} 0 & -Ai & Ai \\ Ai & 0 & -Bi \\ -Ai & Bi & 0 \end{pmatrix}$$

$$\hat{Q}_{yz} = \begin{pmatrix} 0 & A'i & -A'i \\ -A'i & 0 & B'i \\ A'i & -B'i & 0 \end{pmatrix}$$

where the $A^{(\prime)}$ terms mix the singlet with the doublet states, and the $B^{(\prime)}$ terms split the doublet. It has been demonstrated that the dominant order parameter in the quadrupolar phase $T_{+1} < T < T_0$ is Q_{zx}, and the heat capacity measurements require B' to be approximately zero [8]. Although we are unable to probe the phase between T_{+1} and T_{-1} using azimuthal XRS, measurements of the temperature dependence reveal scattering only at (103) in this temperature range, and the absence of a large change in entropy is consistent with the onset of a Q_{yz} component to the quadrupolar order with an anti-phase stacking along to c-axis. The large change in entropy at T_{-1}, assuming that Q_{xy} is the dominant order parameter, requires that the value of B in the matrix is non-zero. As with the symmetry argument in the phase $T_{+1} < T < T_0$, where a non-zero expectation value for Q_{zx} will induce a finite value for $Q_{x^2-y^2}$, because the tensors for Q_{xy} and Q_{yz} have the same symmetry, we anticipate that at the T_{-1} transition there will be an additional, secondary, Q_{yz} component to the quadrupolar order. In this case, the Q_{yz} quadrupoles would be stacked in-phase along the c-axis.

From an examination of the $\sigma\sigma$ data alone, it is not possible to identify definitively whether there is an admixture of Q_{yz} in the scattering tensor below T_{-1}, since, as shown in figures 7(c) and (d), the $\sigma\sigma$ scattering for Q_{xy} and Q_{yz} order displays the same azimuthal dependence. However, the azimuthal dependences of $\sigma\pi$ scattering for the two quadrupolar scattering tensors show very different periodicity and modulation, and therefore it might be possible to deduce the presence of a Q_{yz} component to the scattering. When a simultaneous least squares fit is made to the two scattering channel data sets, allowing the Q_{xy} and Q_{yz} components of the scattering tensor to vary freely, we find that the best fit is obtained for Q_{xy} and Q_{yz} in the ratio 14:1. Such an admixture of Q_{yz} makes only a very small difference in the calculated azimuthal dependence of the scattered intensity, with a change in the relative heights of the peaks at $\Psi = -90°$, $0°$, $90°$.

Similarly in the lowest temperature phase, the calculations indicate that this phase can be described simply using the

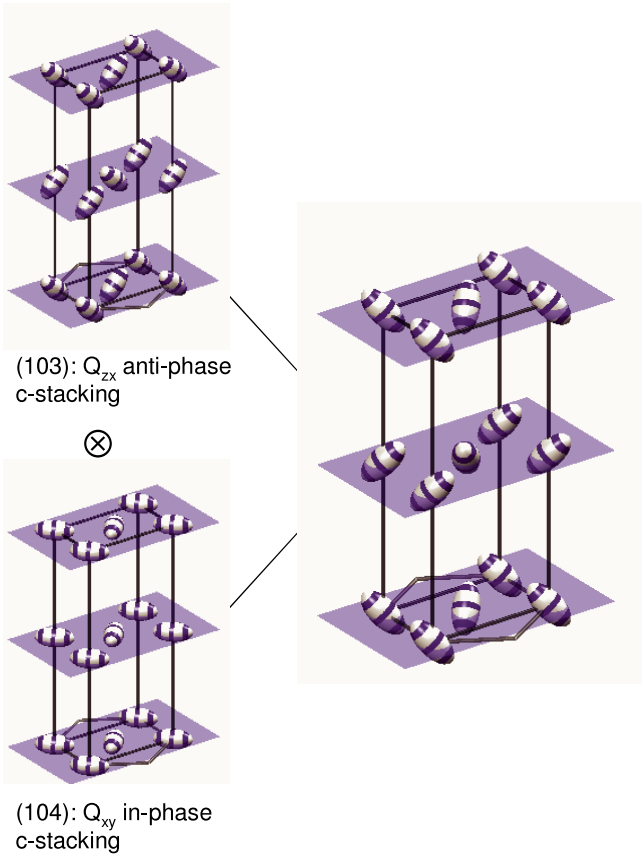

Figure 8. Orthorhombic UPd_3 unit cell showing quadrupolar charge distributions on the quasi-cubic uranium sites as described by the anti-phase c-stacking Q_{zx} and in-phase c-stacking Q_{xy} order parameters.

Q_{xy} order parameter, see figure 6. However, the temperature dependence of the scattered intensity at (104) exhibits a significant increase at T_2 [18], and this is also shown by the change in the relative intensities above and below T_2 as in figures 5 and 6. When a least squares fit is made to the $\sigma\sigma$ and $\sigma\pi$ data sets, we find that the ratio of Q_{xy} to Q_{yz} has changed to 8:1, indicating that the T_2 transition is associated with an increase in the Q_{yz} order parameter, suggesting a rotation of the quadrupole moments about the x-axis.

5. Conclusions

From the x-ray resonant scattering experiments reported in this paper, we have conclusively identified the dominant order parameter describing the component with in-phase stacking along the c-axis of the antiferroquadrupolar structures in the phases $T_2 < T < T_{-1}$ and $T < T_2$ to be Q_{xy}. Further analysis of the azimuthal data using the symmetries of the quadrupolar operators for the three-level crystal field model indicates a small admixture of Q_{yz}.

In summary, these and our previous experiments [8] have allowed us to identify the following sequence of successive quadrupolar transitions in UPd_3: (a) below $T_0 = 7.8$ K the primary order parameter is Q_{zx} with a secondary admixture of $Q_{x^2-y^2}$ describing an antiferroquadrupolar structure with anti-phase stacking along the c-axis; (b) below $T_{+1} = 6.9$ K there is a Q_{yz} component to the above structure; (c) below $T_{-1} = 6.7$ K there is an onset of in-phase stacking along the c-axis, which is primarily described by the Q_{xy} order parameter, but with a secondary admixture of Q_{yz}; (d) below $T_2 = 4.4$ K the admixture of the Q_{yz} component increases in magnitude.

Acknowledgments

We thank Des McMorrow for his invaluable advice, especially during the early stages of our experiments. We are most grateful to all the staff, past and present, at the ID20 beamline for their assistance and advice, particularly Blanka Detlefs, Carsten Detlefs, Andrea Fondacaro, Claudio Mazzoli and Stuart Wilkins. HCW and MDL thank the UK Engineering and Physical Sciences Research Council for the provision of research studentships.

References

[1] Link P, Gukasov A, Mignot J-M, Matsumura T and Suzuki T 1998 *Phys. Rev. Lett.* **80** 4779
[2] Tokura Y and Nagaosa N 2000 *Science* **288** 462
[3] Gehring G and Gehring K 1975 *Rep. Prog. Phys.* **38** 1
[4] Sera M, Ichikawa H, Yokoo T, Akimitsu J, Nishi M, Kakurai K and Kunii S 2001 *Phys. Rev. Lett.* **86** 1578
[5] Santini P, Carretta S, Magnani N, Amoretti G and Caciuffo R 2006 *Phys. Rev. Lett.* **97** 207203
[6] Park J-G, Adroja D T, McEwen K A, Kohgi M and Iwasa K 2008 *Phys. Rev.* B **77** 085102
[7] Morin P and Schmitt D 1990 *Ferromagnetic Materials* vol 5 (Amsterdam: North-Holland) pp 1–132
[8] Walker H C, McEwen K A, McMorrow D F, Wilkins S B, Wastin F, Colineau E and Fort D 2006 *Phys. Rev. Lett.* **97** 137203
[9] Heal T J and Williams G I 1955 *Acta Crystallogr.* **8** 494
[10] McEwen K A, Walker H C, Le M D, McMorrow D F, Colineau E, Wastin F, Wilkins S B, Park J-G, Bewley R I and Fort D 2007 *J. Magn. Magn. Mater.* **310** 718
[11] Steigenberger U, McEwen K A, Martinez J L and Fort D 1992 *J. Magn. Magn. Mater.* **108** 163
[12] Zochowski S W, de Podesta M, Lester C and McEwen K A 1995 *Physica* B **206/207** 489
[13] Tokiwa Y, Sugiyama K, Takeuchi T, Nakashima M, Settai R, Inada Y, Haga Y, Yamamoto E, Kindo K, Harima H and Ōnuki Y 2001 *J. Phys. Soc. Japan* **70** 1731
[14] McEwen K A, Park J-G, Gipson A J and Gehring G A 2003 *J. Phys.: Condens. Matter* **15** S1923
[15] Zochowski S W and McEwen K A 1994 *Physica* B **199/200** 416
[16] Lingg N, Maurer D, Müller V and McEwen K A 1999 *Phys. Rev.* B **60** R8430
[17] McEwen K A, Steigenberger U, Clausen K N, Park J-G, Kulda J and Walker M B 1998 *J. Magn. Magn. Mater.* **177–181** 37
[18] McMorrow D F, McEwen K A, Steigenberger U, Rønnow H M and Yakhou F 2001 *Phys. Rev. Lett.* **87** 057201
[19] Walker H C, McEwen K A, Boulet P, Colineau E, Griveau J-C, Rebizant J and Wastin F 2007 *Phys. Rev.* B **76** 174437
[20] Gibbs D, Harshman D R, Isaacs E D, McWhan D B, Mills D and Vettier C 1988 *Phys. Rev. Lett.* **61** 1241

[21] Beale T A W, Spencer P D, Hatton P D, Wilkins S B, Zimmermann M v, Brown S D, Prabhakaran D and Boothroyd A T 2005 *Phys. Rev.* B **72** 064432
[22] Wilkins S B, Caciuffo R, Detlefs C, Rebizant J, Colineau E, Wastin F and Lander G H 2006 *Phys. Rev.* B **73** 060406
[23] Santini P, Carretta S, Amoretti G, Caciuffo R, Magnani N and Lander G H 2008 *Rev. Mod. Phys.* submitted
[24] Wilkins S B, Paixão J A, Caciuffo R, Javorsky P, Wastin F, Rebizant J, Detlefs C, Bernhoeft N, Santini P and Lander G H 2004 *Phys. Rev.* B **70** 214402
[25] Fort D 1997 *Rev. Sci. Instrum.* **68** 3504
[26] Paolasini L, Detlefs C, Mazzoli C, Wilkins S, Deen P P, Bombardi A, Kernavanois N, de Bergevin F, Yakhou F, Valade J P, Breslavetz I, Fondacaro A, Pepellin G and Bernard P 2007 *J. Synchrotron Radiat.* **14** 301